CHAPTER 268

Asymmetric and Irregular Wave Effects on Bedload: Theory versus Laboratory and Field Experiments

Leszek M. Kaczmarek & Rafał Ostrowski[1]

1. INTRODUCTION

To parameterise the sediment transport in terms of the wave spectrum and a few other parameters, it is necessary to start from the surface elevation spectrum which can be transformed into orbital velocities at the bed and then to bed shear stress. The bed shear stress so derived is used in a new sediment transport formula put forth by the Authors. The problem is highly non-linear and at a few points in the process it is necessary to make non-linear transformations. This route: surface elevation - sediment transport and the importance of the non-linearity are central to this study.

The theoretical model is based on the concept proposed by Kaczmarek & O'Connor (1993) who used the procedure for matching the solutions of equation of motion in the turbulent flow above the theoretical bed level and in the collision-dominated granular-fluid region. This concept, first used for regular linear waves, has recently been developed for random waves by Kaczmarek et al. (1994) and for non-linear waves by Kaczmarek (1995).

Then, on the above basis, the first attempt was made by Kaczmarek et al. (1995) to formulate bedload theory and verify it using available laboratory data and IBW PAN radio-tracer field results.

This paper presents the results of experiment carried out at IBW PAN laboratory. The verification of the theory for regular and irregular waves using own experimental data is the major goal of this study. There are few experimental data sets for ripple regime, especially in the range $\theta_{2.5}$=0.1-0.4. Therefore the laboratory survey covered this range, particularly taking account of the identification of non-linear effects. This range of small $\theta_{2.5}$ is extremely important as one can expect the equivalence of bedload and total sediment transport in this regime (small suspended load rate). Thus,

[1] both Polish Academy of Sciences' Institute of Hydro-Engineering, *IBW PAN*,
7 Kościerska, 80-953 Gdańsk, Poland

only in this regime bedload theory can be precisely verified while in more severe hydrodynamic conditions bedload is a minor part of total sediment transport.

The various aspects of the non-linearity in respect to moveable bed roughness including the asymmetry of waves (described by 2nd and 3rd Stokes theory) and the wave-current interactions as well as wave irregularity are also discussed. A methodology for predicting the bed shear stress time series for irregular waves is applied to a large number of data sets of bottom velocity, some of which are simulated from field free surface elevation spectrum and some taken from IBW PAN laboratory data. The resulting bed shear stress is used in the bedload transport formula to predict sediment transport rate series for each data set. Hence, some questions concerning the equivalent regular waves generating the same shear stress root-mean-square values and the same bedload root-mean-square values as the irregular waves are answered.

2. MOVEABLE BED BOUNDARY LAYER THEORY

2.1. FORMULATION OF THE PROBLEM

The nearbed dynamics is examined and modelled for the flow regions above and beneath the original static bed line, see Figure 1. The collision-dominated granular-fluid region I stretches below the nominal static bed while the wall-bounded turbulent fluid region II extends above it. Since both water and sand grains are assumed to move in both regions, there must be a certain transition zone between I and II, in which the velocity profiles of I and II would merge and preserve continuity of shape.
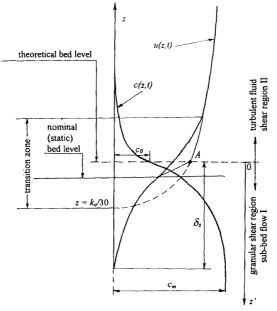

Figure 1. Definition sketch

The velocity distribution about a porous rough bed is controlled by various features of roughness and bed permeability. At first it is assumed that the velocity is determined by roughness geometry and outer flow parameters, such as the free-stream wave velocity.

The iteration procedure permits matching of velocities in the regions I and II. The velocity profile in the upper turbulent layer, which is linked with identification of roughness k_a, is determined first and then passed to the lower collision-dominated layer. The intersection of the two velocity profiles is marked as point A in Figure 1.

2.2. BASIC EQUATIONS

The flow in the turbulent upper region for regular waves is described by the integral momentum model based on the solution proposed by Fredsøe (1984):

$$\frac{dz_1}{d(\omega t)} = \frac{30\kappa^2 U}{k_a \omega e^{z_1}(z_1 - 1) + 1} - \frac{z_1(e^{z_1} - z_1 - 1)}{e^{z_1}(z_1 - 1) + 1} \frac{1}{U} \frac{dU}{d(\omega t)} \tag{1}$$

$$\frac{dz_1}{d(\omega t)} = \frac{30 z_1^2 \left[\left|\frac{\kappa U}{z_1} \mp u_{f0}\right| \left(\frac{\kappa U}{z_1} \pm u_{f0}\right) \pm u_{f0}^2\right]}{k_a \omega U \left[e^{z_1}(z_1 - 1) + 1\right]} - \frac{z_1(e^{z_1} - z_1 - 1)}{e^{z_1}(z_1 - 1) + 1} \frac{1}{U} \frac{dU}{d(\omega t)} \tag{2}$$

for pure wave motion and wave with/against current, respectively.

The solutions of Equations (1) and (2) are achieved by the Runge-Kutta second-order method. As a result for a particular case, the function $z_1(t)$ is obtained and the time distributions of the friction velocity $u_f(t)$ and boundary layer thickness $\delta(t)$ are calculated thereafter using the following equations:

$$z_1 = \frac{U\kappa}{u_f \mp u_{f0}} \tag{3}$$

$$\delta = \frac{k_a}{30}\left(e^{z_1} - 1\right) \tag{4}$$

It should be emphasised that the free stream velocity $U(t)$ can be described as linear or nonlinear, thus Fredsøe's model can be adapted to nonlinear (asymmetric) wave motion, cf. Kaczmarek & Ostrowski (1992).

The solutions of Equations (1) and (2) enable the values of u_{fmax} to be determined, if the quantities k_a are specified. To evaluate the roughness parameter k_a an iterative procedure is proposed for finding the matching point A.

The approach for irregular waves incorporates a time-invariant, two-layer eddy viscosity and bottom boundary layer thickness. Bed roughness is calculated using the iteration procedure taking account of the reduction of this parameter due to irregularity of wave motion. More detailed discussion on modelling of bed roughness is given in section 3.1.

In the sub-bed flow region, the sediment concentration is high and chaotic collisions of grains are the predominant mechanism. Particle interactions are assumed to produce two distinct types of behaviour. The Coulomb friction between particles give rise to rate-independent stresses (of the plastic type) and the particle collisions bring

about stresses that are rate-dependent (of the viscous type). The use of the mathematical description by Sayed & Savage (1983) for determination of the stress tensor was made and the balance of linear momentum according to Kaczmarek & O'Connor (1993) leads to the following equations:

$$\alpha^0 \left(\frac{c - c_0}{c_m - c} \right) \sin\varphi \sin 2\psi + \mu_1 \left(\frac{\partial u}{\partial z'} \right)^2 = \rho u_f^2 \tag{5}$$

$$\alpha^0 \left(\frac{c - c_0}{c_m - c} \right) \left(1 - \sin\varphi \sin 2\psi \right) + \left(\mu_0 + \mu_2 \right) \left(\frac{\partial u}{\partial z'} \right)^2 = $$
$$\left(\frac{\mu_0 + \mu_2}{\mu_1} \right)\Bigg|_{c=c_0} \rho u_f^2 + \left(\rho_s - \rho \right) g \int_0^{z'} c \, dz' \tag{6}$$

in which:

ρ_s and ρ are the densities of the solid and fluid, respectively;

α^0 is a constant;

c_0 and c_m are the solid concentrations corresponding to fluidity and the closest packing, respectively;

μ_0, μ_1 and μ_2 are functions of the solid concentration c:

$$\frac{\mu_1}{\rho_s d^2} = \frac{0.03}{(c_m - c)^{1.5}} \tag{7}$$

$$\frac{\mu_0 + \mu_2}{\rho_s d^2} = \frac{0.02}{(c_m - c)^{1.75}} \tag{8}$$

The value φ in Equations (5) and (6) is the quasi-static angle of internal friction, while the quantity ψ is equal to:

$$\psi = \frac{\pi}{4} - \frac{\varphi}{2} \tag{9}$$

For the calculations the following numerical values are recommended:

$$\frac{\alpha^0}{\rho_s g d} = 1 \qquad c_0 = 0.32 \qquad c_0 = 0.32 \qquad \varphi = 24.4° \tag{10}$$

where d denotes the diameter of grains.

3. MODELLING OF BEDLOAD UNDER IRREGULAR WAVES

3.1. BED ROUGHNESS

The apparent bed roughness parameter k_a is a central quantity in the theoretical model. Both the turbulent and sub-bed velocity profiles depend on k_a, which is not known a priori. Therefore an iteration procedure is proposed for finding the matching point A between these profiles. The matching is assumed to take place at the phase of maximum shear stress, although at any other phase of oscillatory motion there must be some transition between the two profiles. Under monochromatic waves the maximum shear stress is the maximum value of shear stress during a wave period, while for spectral waves it becomes the maximum value of the random shear stress

time series. To calculate this value it is proposed to use, the following simple relation, Kaczmarek et al. (1994):

$$\tau_{max} = \frac{3\tau_{rms}}{\sqrt{2}} = 3\delta_\tau \tag{11}$$

The choice is fairly arbitrary, however, as it was shown by Kaczmarek et al. (1994), it yields the best agreement of the calculations of wave friction using Madsen et al.'s (1990) data.

For engineering purposes it is useful to approximate the theoretical results by a curve expressed in terms of skin friction. To determine the skin friction one can follow Nielsen's (1992) description:

$$\theta_{2.5} = \frac{1}{2} f_{2.5} \ \psi_1 = \frac{1}{2} f_{2.5} \frac{(a_{1m}\omega)^2}{(s-1)gd} \tag{12}$$

$$f_{2.5} = \exp\left[5.213 \left(\frac{2.5d_{50}}{a_{1m}} \right)^{0.194} - 5.977 \right] \tag{13}$$

in which $s = \rho_s/\rho$.

The iteration procedure proposed for finding the matching point A between the velocity profiles (Fig. 1) was run for a wide range of small and large scale conditions and for a few diameters of sandy bed. Then the results were approximated yielding the following formulae for regular and irregular waves, respectively:

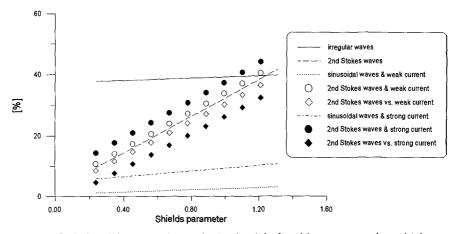$$\frac{k_a}{d} = 47.03\theta_{2.5}^{-0.66} \tag{14}$$

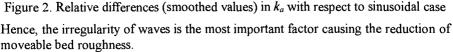$$\frac{k_a}{d} = 26.64\theta_{2.5}^{-0.71} \tag{15}$$

For irregular waves k_a is calculated using Eq. (15) taking root-mean-square wave height (or free-stream velocity) and peak period for determination of $\theta_{2.5}$.

The moveable bed roughness under sinusoidal and asymmetric waves with/versus a steady current has also been considered. The numerical solution of Eq. (2) is used with the free stream velocity $U(\omega\ t)$ expressed using linear or nonlinear approximation. The considerations on nonlinearity have been limited to the 2nd Stokes wave propagating without current and with/against weak and strong currents. For wave-current motion the ratio U_{mean}/U_{1m} was kept constant and amounted to 0.2 and 0.5 for weak and strong current, respectively. The quantity U_{mean} is the steady current, known as an input, averaged over water depth in the outer region (outside the bed boundary layer). The mean slip velocity (at the top of the bed boundary layer) is calculated from U_{mean} with the assumption of the logarithmic velocity profile in the outer region, using the model of Kaczmarek & Ostrowski (1992). This model also provides the value of shear stress u_{f0} resulting from the presence of steady current.

Figure 2 depicts the relative differences in roughness computed for regular waves (linear and nonlinear) and currents, as well as irregular wave motion, with respect to pure sinusoidal cases. The results imply that the greatest reduction of the roughness

parameter k_a (about 40%) is observed when the waves are irregular and in a certain range of Shields parameter - when the nonlinear waves are accompanied by a steady current. Smaller reductions of k_a occur for sinusoidal waves superimposed on currents. It can be seen that for nonlinear cases the reduction of k_a is more distinct for waves propagating with the current than for waves versus the current.

Figure 2. Relative differences (smoothed values) in k_a with respect to sinusoidal case

Hence, the irregularity of waves is the most important factor causing the reduction of moveable bed roughness.

3.2. SHEAR STRESS AND BEDLOAD

It is convenient to introduce complex notation which determines the dependence of velocity on time and will ensure the analytical solution of the equation of motion. The free stream velocity will be written as $U(t)=U\exp(i\omega t)$, in which U = real velocity amplitude. Similarly, one may write:

$$u(z,t) = u(z)e^{i\omega t} \qquad \text{and} \qquad u_d(z,t) = u_d(z)e^{i\omega t} \qquad (16)$$

in which $u(z)$ and $u_d(z)$ are in general complex due to the phase shift relative to the free stream velocity. The equation of motion may now be written as:

$$\frac{d}{dz}\left[v_t(z)\frac{du_d(z)}{dz} \right] - i\omega u_d(z) = 0 \qquad (17)$$

It is fortunate that this equation is explicitly solvable both when $v_t(z)$ varies linearly with z and when it is a constant. Thus, following Brevik (1981), the two-layer eddy viscosity model is proposed:

$$v_t(z) = \kappa u_{fr} z \qquad \text{for} \qquad \frac{k_a}{30} < z \leq \frac{\delta_r}{4} + \frac{k_a}{30} \qquad (18)$$

$$v_t(z) = \kappa u_{fr}\left(\frac{\delta_r}{4} + \frac{k_a}{30} \right) \qquad \text{for} \qquad z > \frac{\delta_r}{4} + \frac{k_a}{30} \qquad (19)$$

where $u_{fr} = \sqrt{\tau_r / \rho}$ and δ_r are the representative friction velocity and representative bottom boundary layer thickness, respectively.

To solve the Eq. (17) the free stream velocity is specified as that associated with a wave spectrum, i.e.:

$$U(t) = \sum_n U_n e^{i\omega_n t} \tag{20}$$

in which the index n denotes summation over frequencies. With such a representation of $U(t)$ the velocity amplitudes U_n are related to the near-bottom orbital velocity spectrum and to the surface amplitude spectrum through:

$$U_n = \sqrt{2S_U(\omega_n)d\omega} = \frac{\omega_n}{\sinh(k_n h)} \sqrt{2S_\eta(\omega_n)d\omega} \tag{21}$$

in which ω_n and k_n are related to each other by linear dispersion relationship.

The linearity of Eq. (17) combined with the assumed time-invariant eddy viscosity concept (Equations (18) and (19)) suggests a solution in the form of:

$$u(z,t) = \sum_n u_n(z) e^{i\omega t} \tag{22}$$

in which $u_n(z)$ represents the complex velocity component amplitudes and only the real part of Eq. (22) constitutes the solution sought.

Introducing Equations (18) and (19) into Equation (17), one can obtain the equation for each velocity component n. Introducing the dimensionless variable:

$$\xi_n = \left(4\omega_n \frac{z}{\kappa u_{fr}} \right)^{\frac{1}{2}} \tag{23}$$

Eq. (17) reduces to the standard differential equation for the Kelvin functions of zeroth order, with ξ_n as the independent variable.

On the basis of the velocity solution one can obtain the shear stress at $z=z_0$ (complex value) which can be expressed as:

$$\tau(t) = \tau_n \exp[i(\omega_n t + \varphi_{\tau n})] \tag{24}$$

where τ_n and $\varphi_{\tau n}$ are the bed shear stress amplitude and phase, respectively, corresponding to nth harmonic component U_n of the input free stream velocity random series $U(t)$.

The solution obtained for the turbulent flow in the wave boundary layer involves the representative friction velocity u_{fr} and the representative thickness of the boundary layer δ_r, which are yet to be specified. Although each harmonic component of wave motion is described by the same equation, i.e. Equation (17), there is a coupling between the components incorporated in the eddy viscosity. This appears in the modelling of the representative values u_{fr} and δ_r by iterative procedure which is schematically shown in Figure 3. The quantities u_{fr} and δ_r are determined by using Eq. (1) and specified as:

$$u_{fr} = u_{f\max} \tag{25}$$

$$\delta_r = \delta_m = \max(\delta_1, \delta_2) \tag{26}$$

where u_{fmax} is the maximum value of bed shear velocity during the wave period, that is $\max[u_f(\omega\ t)]$ and δ_1 and δ_2 the boundary layer thicknesses at the moments corresponding to maximum and minimum velocity at the top of the turbulent boundary layer. For a given by free stream irregular series the iterative procedure of Fig. 3 is used to determine the representative period T_r, friction velocity u_{fr} and the boundary layer thickness δ_r. The exemplary shear stress results vs. Gdańsk lab data, collected by Ostrowski (1993), are shown in Figure 4.

$<1>$	Fourier decomposition of the free stream velocity input $U(t)$ $$U(t) = \sum_n U_n \sin(n\omega t + \varphi_n) + \tfrac{1}{2}U_0$$
$<1a>$	*Alternatively* Fourier decomposition of the water surface elevation input $\eta(t)$ $$U(t) = \sum_n \eta_n \frac{n\omega}{\sinh(k_n h)} \sin(n\omega t + \varphi_n) + \tfrac{1}{2}U_0$$
$<2>$	Calculation of the input root mean square value: $$U_{rms} = \sqrt{\sum_n U_n^2}$$
$<3>$	Computation of bed roughness for irregular waves
$<4>$	Assumption of representative period T_r
$<5>$	Determination of parameters of representative eddy viscosity distribution: u_{fr} & δ_r (running Fredsœ's (1981) model with U_{rms} & T_r as an input)
$<6>$	Computation of representative shear stress amplitude ρu_{fB}^2 (using Brevik's (1981) approach with U_{rms}, T_r & eddy viscosity distribution from step $<5>$ as an input)
$<7>$	Computation of bed shear stress components τ_n & $\varphi_{\tau n}$ using Brevik's approach with U_n, $n\omega$ (from step $<1>$ or $<1a>$) and representative eddy viscosity (determined in step $<5>$) as an input
$<8>$	Calculation of bed shear stress root mean square value: $$\tau_{rms} = \sqrt{\sum_n \tau_n^2}$$
$<9>$	Checking whether ρu_{fB}^2 (step $<6>$) $= \tau_{rms}$ (step $<7>$) if NO $\longrightarrow$ correction of T_r and going to step $<5>$ if YES $\longrightarrow$ going to step $<10>$
$<10>$	Calculation of output time series (bed shear stress): $$\rho u_f^2(t) = \tau(t) = \sum_n \tau_n \sin(n\omega t + \varphi_n + \varphi_{\tau n})$$
$<11>$	Calculation of bedload time series using present model with the boundary conditions $u_f\big|_{z'=0} = u_f(t)$

Figure 3. Computation of bed shear stress and bedload under irregular waves

Once the bed shear stress is determined the velocity distributions can be computed for the regions I and II (Fig. 1), as well as the concentration of grains in bedload layer. Basing on Bagnold's (1956) definition, according to which the bedload is a part of sediment transport subject to inter-granular forces, the bedload layer can be

represented as the region II. Knowing the instantaneous shear stress one can calculate the instantaneous bedload rate from velocity and concentration profiles in this layer:

$$Q_B = \int_0^{\delta_s} u(z',t) \cdot c(z',t)\, dz' \tag{27}$$

and the dimensionless bedload rate defined as:
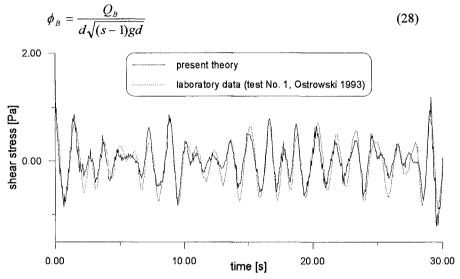
$$\phi_B = \frac{Q_B}{d\sqrt{(s-1)gd}} \tag{28}$$

Figure 4. Theoretical and experimental irregular shear stress

The methodology for predicting the bedl oad time series for irregular waves was applied to a number of laboratory data sets. These results are discussed in the next section. The presented concept was also used for modelling of the bedload series for the field free surface elevation series taken at IBW PAN Coastal Research Facility in Lubiatowo. The exemplary results of the bedload simulation are given in Figures 5 and 6.
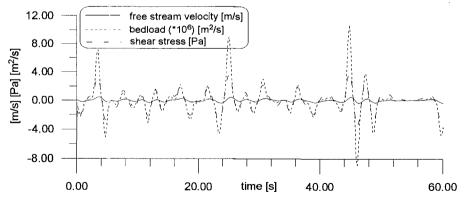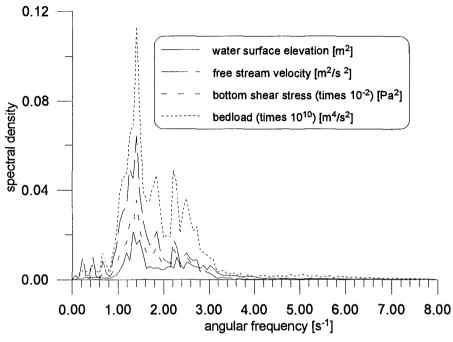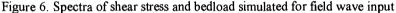

Figure 5. Time series of shear stress and bedload simulated for field wave input

Figure 6. Spectra of shear stress and bedload simulated for field wave input

4. LABORATORY BEDLOAD SURVEY

4.1. EXPERIMENTAL SETUP

The measurements were carried out in the IBW PAN wave flume. The wave flume, 0.5 m wide and 22.5 m long, is equipped with a programmable wave maker and can be filled with water up to 0.7 m. Reinforced concrete slabs 8 cm thick were placed on the bottom with a sandy measuring section (also 8 cm thick) 7 m long situated about the middle of the flume. Natural sand was used in the experiments with a grain diameter d_{50}=0.22 mm.

For each test, free surface elevation was registered at three points along the flume. The horizontal component of free stream velocity was measured at one point in the measuring section, using a micro-propeller, together with one of the wave gauges which was located above the sand trap. The other two wave gauges were spaced $1/4*L$ from each other (L being a wave length) to estimate the reflection effects in the flume. Experimental setup, together with the sand trap, is shown in Figure 7.

The sand trap was covered by a lid and buried in the sandy section before each test. Then the waves were generated until bed ripples were fully formed, which took 25-60 minutes. The lid, suspended on four strings, was removed thereafter, together with a thin layer of sand on it. Then the wave action was continued for 1.2-15 minutes and

sediment grains were being accumulated in the sand trap. Finally, the grains were siphoned from the trap and weighed to determine the sedimentation quantity.

The sand trap had two cells to ensure the determination of onshore and offshore bedload components.

Together with the sedimentation, bed forms geometry was measured and their shape was assessed after each test.
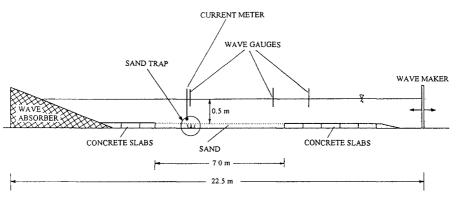

Figure 7. Experimental setup

A constant water depth of $h = 0.5$ m above the measuring section was maintained during each test. The experiments were carried out for six sets of parameters for regular waves (Tests 1, 2, 3, 4, 11 and 12) and for six irregular wave series (Tests 5, 7, 8 for JONSWAP and Tests 6, 9, 10 for Pierson-Moskowitz spectrum generated by the wave maker). As a total, 141 series were run, among which 103 ones were regular.

The conditions expressed in terms of $\theta_{2.5}$ varied roughly from 0.1 in Test 3 to 0.4 in Test 12. This range of rippled bed (cf. Fig. 4b) is extremely important as one can expect the equivalence of bedload and total sediment transport in this regime (small suspended load rate). Thus, only in this regime bedload theory can be precisely verified while in more severe hydrodynamic conditions bedload is a minor part of total sediment transport.

4.2. RESULTS OF MEASUREMENTS VS. PRESENT THEORY

The experimental bedload data in comparison with theoretical results obtained by using present theoretical linear approach are shown in Figure 8.

The waves registered in the flume had a slightly asymmetric shape. Therefore, for better representation of actual laboratory conditions, the theoretical results have been produced using present approach adapted for non-linear waves. The free stream velocity in Equation (1) was described using 2nd order Stokes theory, as indicated by Kaczmarek & 'Ostrowski (1992). Then, for known distributions of u_f in time, the instantaneous bedload transport rate has been found from Equations (5) and (6) for

the entire wave period, integrated over time and averaged over wave period. These results are also shown in Figure 8.

The conformity of theoretical evaluations and experimental data can be seen in Figure 8, especially while using non-linear approach (except for Test 2). It should be pointed out that for long and highly asymmetric waves, represented by Test 11 (Ursell parameter of 40), the experimental data fit the present non-linear theory while they differ significantly from the linear approach. The most severe shear stress conditions generated in the flume without wave breaking had a $\theta_{2.5}=0.4$ and were achieved in Test 12. However, the Ursell number (equalled to 31) was less than in Test 11. In Test 12, a very distinct concentration of suspended sediment was observed which could result in increased accumulation in the sand trap, bigger than theoretically modelled, using both linear and non-linear theory.
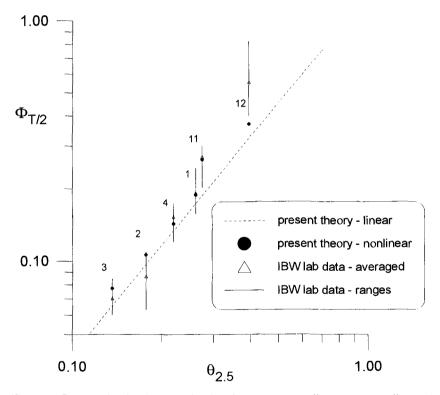

Figure 8. Regular bedload IBW PAN lab data vs. present linear and non-linear theory

The laboratory bedload data for irregular waves in comparison with theoretical results are depicted in Figure 9. Computed values have been modelled using the present computational procedure (Fig. 3) for the full-time (15 minutes) water surface elevation series registered at the measuring section. The agreement between theoretical and experimental results appears to be very good.
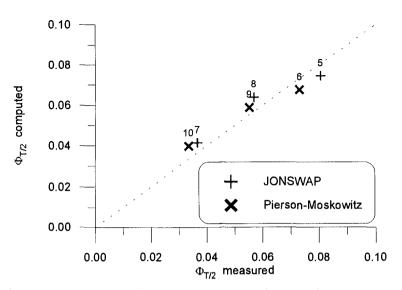
Figure 9. Bedload IBW PAN lab data vs. present theory for irregular waves

For the sake of full comparison the laboratory bedload data for regular and irregular waves are plotted together in Figure 10, against linear theory. Additionally, the bedload results simulated for field-recorded waves are included in Fig. 10. All results for irregular waves are presented as a function of dimensionless stress $\theta_{2.5}$, calculated using root-mean-square wave height and representative wave period T_r.
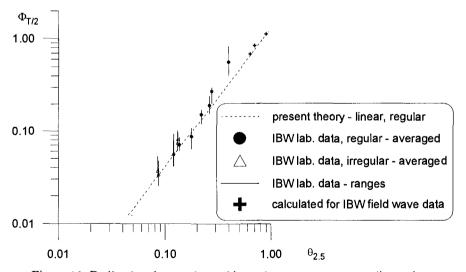

Figure 10. Bedload under regular and irregular waves vs. present linear theory

Figure 10 implies that the bedload rate for irregular cases can be successfully modelled with the use of present linear theory taking root-mean-square wave height

H_{rms} and representative wave period T_r as an input. It should be noted that in analysed cases the computed values of T_r are close to those of peak period, thus the peak period (T_p) can be used as representative. However, further studies are necessary to find out whether this conclusion is valid for all types of spectra.

It can also be seen from Figure 10 that for weak and moderate shear stress conditions the regular laboratory bedload data lie slightly above the results obtained using linear theory, thus for precise determination of bedload rate under regular-asymmetric waves the non-linear approach should be used. Finally, it can be concluded that for high shear stresses the present linear theory underestimates bedload rate, most probably - due to significant concentration of suspended sediment.

REFERENCES

Bagnold, R.A. (1956). The flow of cohesionless grains in fluids, *Phil. Trans.*, R. Soc., London, Ser. A, 249 (964), 235-297

Brevik, I. (1981). Oscillatory Rough Turbulent Boundary Layers, *J. Wtrway., Port, Coast. and Oc. Eng.*, ASCE, Vol. 107, No. 3, 175-187

Fredsøe, J. (1984). Turbulent boundary layer in combined wave-current motion, *J. Hydraulic Eng.*, ASCE, Vol. 110, No. HY8, 1103-1120

Kaczmarek, L.M. (1995). Nonlinear Effects of Waves and Currents on Moveable Bed Roughness and Friction, *Archives of Hydro-Engineering and Environmental Mechanics*, Vol. 42, No. 1-2, pp. 3-27

Kaczmarek, L.M., J.M. Harris & B.A. O'Connor (1994). Modelling moveable bed roughness and friction for spectral waves, *Proc. 24th ICCE*, 300-314, ASCE, New York

Kaczmarek, L.M. and B.A. O'Connor (1993a, b). A new theoretical approach for predictive evaluation of wavy roughness on a moveable flat/rippled bed, Parts I/II, *Reps. CE/*14-15/93, Dept. Civ. Engng., Univ. Liverpool

Kaczmarek, L.M. and Ostrowski, R. (1992). Modelling of wave-current boundary layer in the coastal zone, *Proc. 23rd Intern. Conf. Coast. Eng.*, ASCE, 350-363

Kaczmarek, L.M., R. Ostrowski & R.B. Zeidler (1995). Boundary Layer Theory and Field Bedload, *Proc. International Conf. Coast. Res. in Terms of Large Scale Experiments (Coast. Dynamics '95)*, ASCE, 664-675

Madsen, O.S., P.P. Mathison & M.M. Rosengaus (1990). Moveable bed friction factors for spectral waves, *Proc. 22nd Intern. Conf. Coast. Engng.*, 420-429, ASCE, New York

Nielsen, P. (1992). Coastal bottom boundary layers and sediment transport. *Advanced Series on Ocean Engineering*, Vol. 4, World Scientific, Singapore

Ostrowski, R. (1993). Bottom friction induced by surface waves and currents with nonlinear effects (in Polish), *Ph. D. thesis*, IBW PAN, Gdańsk

Sayed, M. and Savage, S.B. (1983). Rapid gravity flow of cohesionless granular materials down inclined chutes, *J. Applied Mathematics and Physics* (ZAMP), Vol. 34, 84-100